PAPER III

Radi Ajjaji

Introduction

4d-var is able to extract information from the observations in a way consistent with the dynamics of the model. Assuming the latter is perfect, it is equivalent to a Kalman filter for the result at the final time; it uses flow-dependent structure functions, though it does not allow them evolve in time explicitly.

A practical way of exhibiting the implicit 4d-var structure functions is to perform a 4d-var assimilation experiment with a single observation : the analysis increments are proportional to the forecast error-covariances between the observed variable at the observation point and all other locations and variables.

Thépaut et al. (1996) have shown how complex forecast error covariances can be when they evolve according to primitive equation dynamics. The shape of the analysis increments provides a three-dimensional picture of the covariances of the background errors modified by the dynamics.

This paper presents a case study analysing the structure functions in 4d-var on a real meteorological situation characterized by a fictitious over-estimation of specific-humidity increments over Spain in the context of Météo-France ARPEGE 4d-var assimilation.

First, the tangent-linear hypothesis is examined in presence of this strange specific humidity feature. Then, a theoretical study, consisting in determining the vector of 4d-var increments when only one single observation is introduced in the cost function, is presented in order to show the different ingredients governing the increments magnitude.

Then, the randomisation technique, discussed by Fisher and Courtier (1995) and used by Anderson et al. (2000), giving global gridpoint values of background-error standard deviations in terms of observable quantities, is used to diagnose the specific-humidity background-error standard deviations involved implicitly in this case study.

1. Test of the tangent-linear hypothesis for the situation of April 24th, 2001

Comparisons were done between, on one hand the evolution over 6 hours of a perturbation (of the order of magnitude of analysis increments) with the simplified tangent-linear (TL) model $M(\delta x)$, and on the other hand the finite difference between two nonlinear forecasts, one from a basic state (x) and the other one from a perturbed state ($x + \delta x$). Theses runs are performed in adiabatic mode with simple linear vertical-diffusion and surface-drag schemes (Buizza, 1994). The perturbation used corresponds to the 4d-var increments resulting from an experiment with a single surface geopotential observation (40.93°N, 1.30°W, 902 m).

On Fig. 1, one can notice that there is no major difference between the adiabatic tangent-linear model and finite differences from the nonlinear model, for temperature and wind fields. Concerning specific humidity, finite differences show a region of large differences, over the Atlantic West of Spain. Intuitively, one can explain that by the lack of physics in the used TL model. But, as shown on Fig. 2, when switching on the entire simplified-physics package (vertical turbulence, gravity wave drag, stratiform precipitations, convection and radiation), the TL model still shows the same features around 20°W.

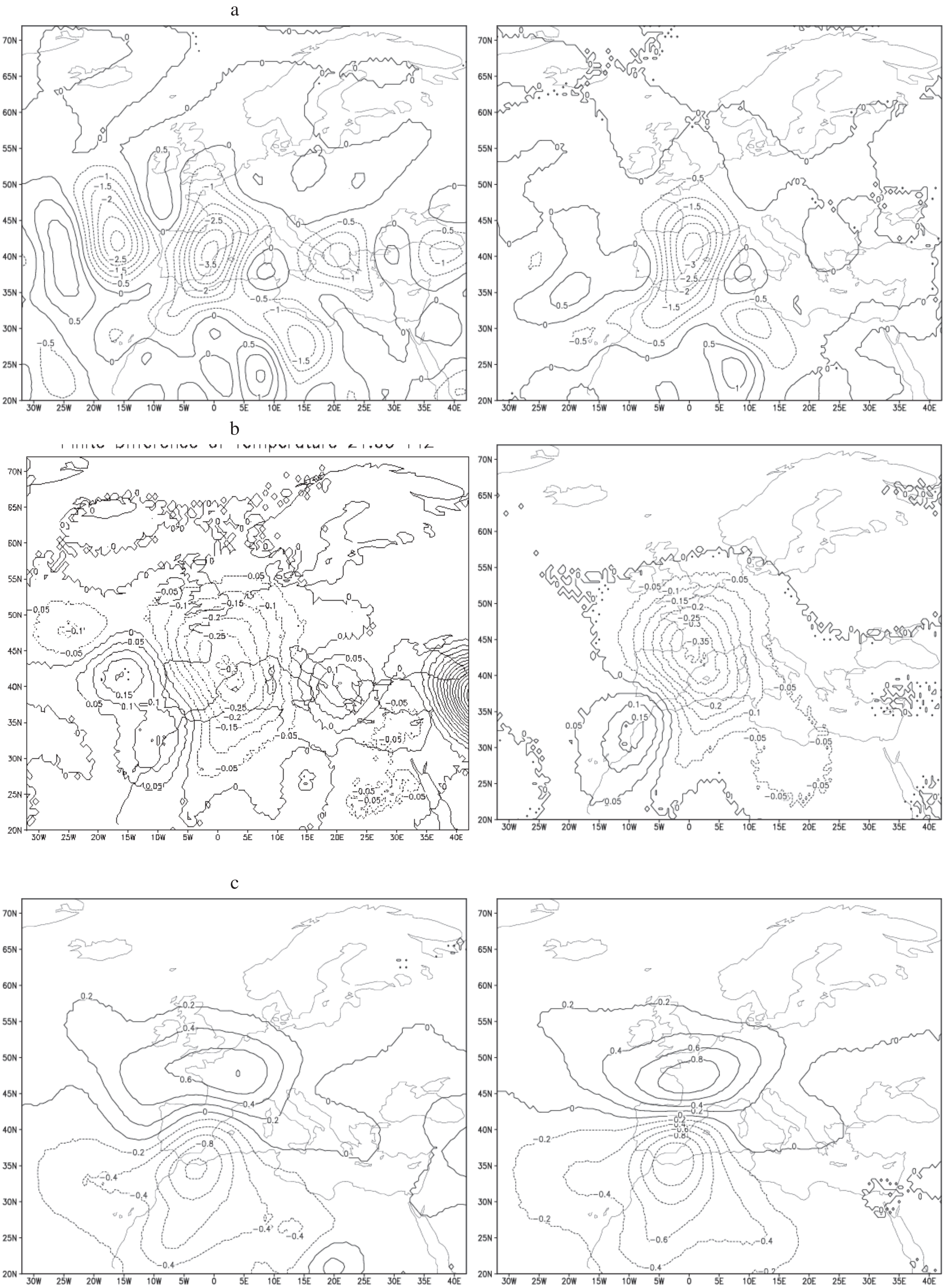

Figure 1: Finite differences (left) and tangent-linear integration (righ, at the end of the assimilation window (i.e. at 21:00 UTC on April 24th, 2001), for : a) specific humidity, b) temperature, c) zonal wind, at 850 hPa (when a single geopotential observation located at [40.93°N,1.30°W, 902 m].is introduced at 18:00 UTC)

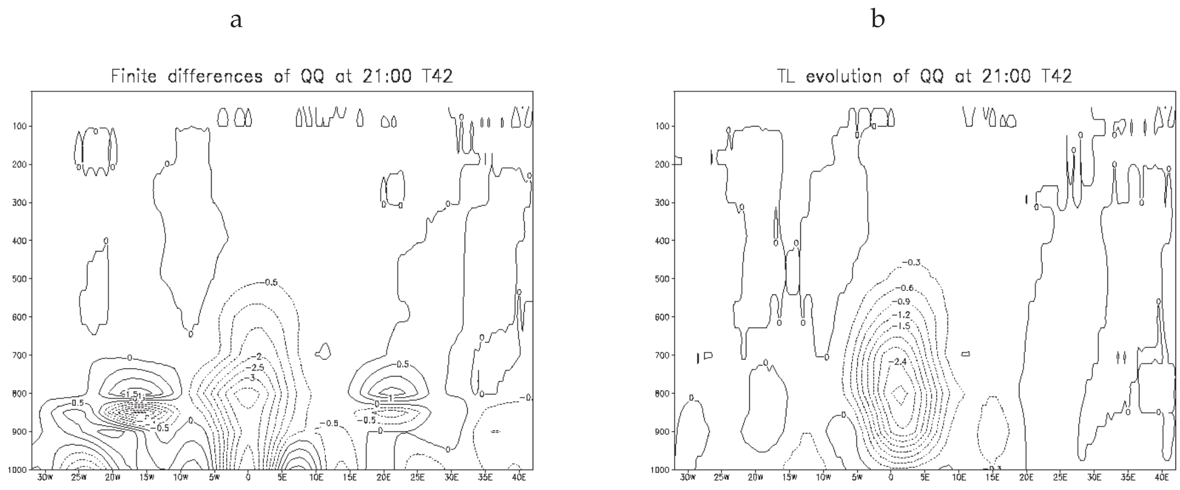

Figure 2: Vertical cross-sections of specific humidity at 42.5°N for : a) finite differences, b) tangent-linear evolution with full simplified physics. The values are multiplied by 10^4 and valid at the end of the assimilation window.

The pattern that appears on the Atlantic is however very local on the vertical : it concerns a small layer between 900 hPa and 800 hPa. Simplified physics is eventually not enough realistic to catch it efficiently. On the other hand, some other localized features appear near to the surface, along the cross-section axis, in the finite differences for specific humidity. They denote certainly, a weakness of the simplified vertical-turbulence scheme.

Concerning the pattern associated to the large increment given by 4d-var analysis over North-West Spain and visible on the cross-sections at the vertical of 0°W, finite differences from the nonlinear evolution of the associated perturbation remain very similar to the TL evolution, on the horizontal and the vertical, despite the existence of a slight difference near the surface. Thus, it appears that the tangent-linear hypothesis is likely not to affect viciously the specific-humidity increments.

The above-discussed results, relative to the context of a single geopotential observation, are also obtained when using a perturbation corresponding to the 4d-var increments implied by the full set of observations (Fig. 3).

2. Theoretical expression of 4d-var specific-humidity analysis increments induced by a single observation

In an analysis (3d-var or O.I. or each analysis step of a Kalman filter), the analysis increments, x^a-x^b, are a linear combination of the innovations, y-$H(x^b)$ (Lorenc, 1986) :

$$\delta x = x^a - x^b = BH'^{T}(H'BH'^{T}+R)^{-1}[y - H(x^b)]$$

where y stands for the vector of observations, x^b for the background, H for the operator which predicts the observations from the model initial state, R for the covariance matrix of observation errors and B for the covariance matrix of background errors; H' is the linearization of H in the vicinity of the background x^b, ^{T} denotes the transpose of a matrix.

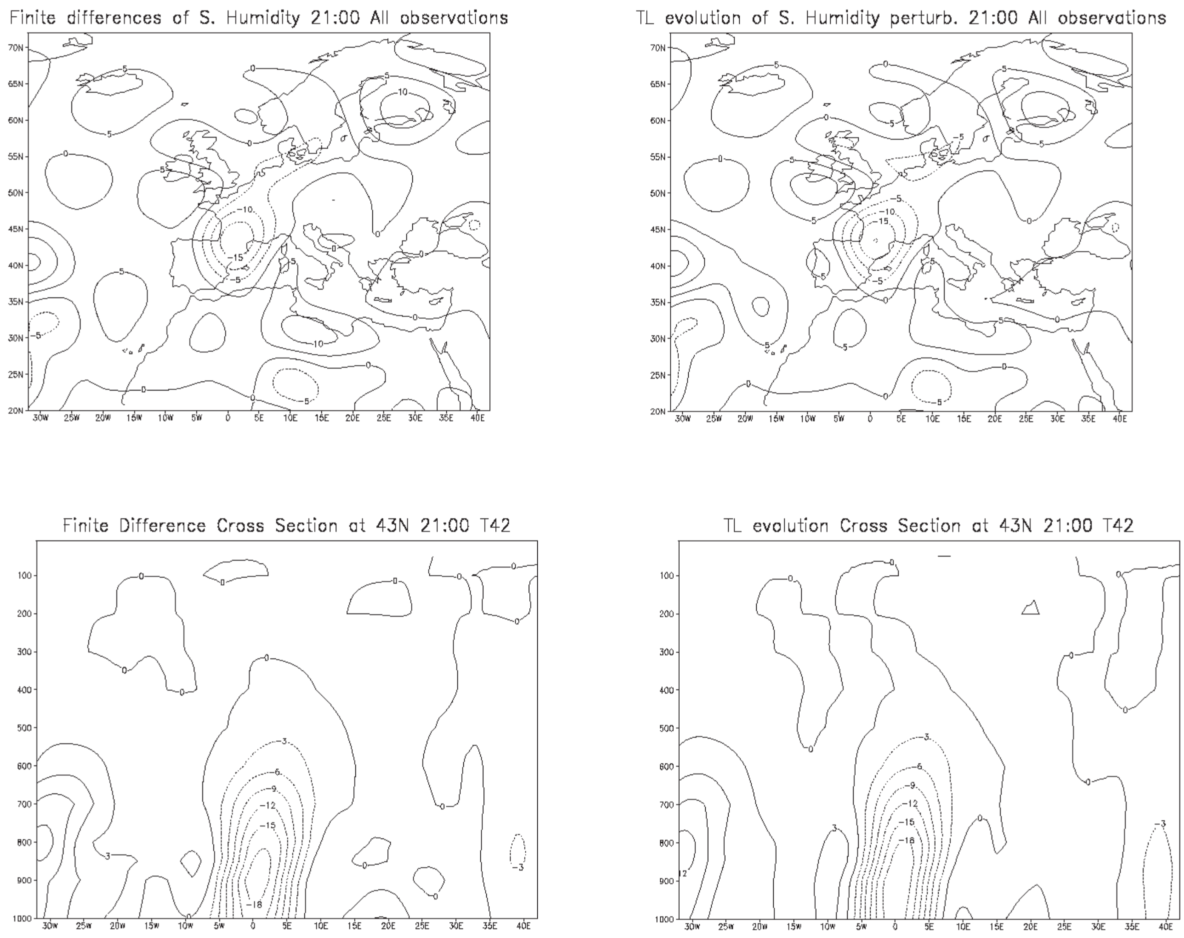

Figure 3: Finite differences (left) versus tangent-linear evolution (right) for specific humidity. The perturbation used corresponds to the 4d-var increments associated to a full set of observations (maps at 850 hPa and vertical cross-sections at 42.5°N).

To simplify the interpretation, we suppose that the state variable x is reduced to five variables : u, v, P, T and q. The temporal step is taken equal to 1 second ($\Delta t = 1$).

On one tangent-linear timestep evolution, we can write :

$$\begin{bmatrix} \vec{u}'(t+1) \\ T'(t+1) \\ q'(t+1) \\ P'(t+1) \end{bmatrix} = M \begin{bmatrix} \vec{u}'(t) \\ T'(t) \\ q'(t) \\ P'(t) \end{bmatrix} \tag{1}$$

where the tangent-linear operator M is given by the following matrix (cf. paper II) :

$$\begin{pmatrix} A_{\vec{u}} & \vec{B}_{\vec{u}} & \vec{C}_{\vec{u}} & \vec{D}_{\vec{u}} \\ \vec{A}_T & B_T & C_T & D_T \\ \vec{A}_q & 0 & C_q & D_q \\ \vec{A}_P & 0 & 0 & D_P \end{pmatrix} \tag{2}$$

If we consider a B matrix in which cross-covariances between different variables are not taken into account, then we have :

$$\mathrm{B} = \begin{pmatrix} \mathrm{B}[\vec{u}'(t)] & 0 & 0 & 0 \\ 0 & \mathrm{B}[T'(t)] & 0 & 0 \\ 0 & 0 & \mathrm{B}[q'(t)] & 0 \\ 0 & 0 & 0 & \mathrm{B}[P'(t)] \end{pmatrix} \tag{3}$$

$$\mathrm{B}M^T = \begin{pmatrix} A_{\vec{u}}\mathrm{B}[\vec{u}'(t)] & \vec{A}_T\mathrm{B}[\vec{u}'(t)] & \vec{A}_q\mathrm{B}[\vec{u}'(t)] & \vec{A}_P\mathrm{B}[\vec{u}'(t)] \\ \vec{B}_{\vec{u}}\mathrm{B}[T'(t)] & B_T\mathrm{B}[T'(t)] & 0 & 0 \\ \vec{C}_{\vec{u}}\mathrm{B}[q'(t)] & C_T\mathrm{B}[q'(t)] & C_q\mathrm{B}[q'(t)] & 0 \\ \vec{D}_{\vec{u}}\mathrm{B}[P'(t)] & D_T\mathrm{B}[P'(t)] & D_q\mathrm{B}[P'(t)] & D_P\mathrm{B}[P'(t)] \end{pmatrix} \tag{4}$$

If we introduce a single wind-observation at time $t+1$ on one particular gridpoint, the observation-operator matrix is then reduced to a row vector containing the value 1 at the gridpoint corresponding to the observation and the value 0 elsewhere.

The matrix BM^TH^T contains then the covariances between $(u',v')(t+1)$ at the observation location and the errors on the five variables at time t. BM^TH^T involves the auto-covariances between the observation point and all the gridpoints :

$$\mathrm{B}M^TH^T = \begin{pmatrix} A_{\vec{u}}\hat{\mathrm{B}}[\vec{u}'(t)] \\ \vec{B}_{\vec{u}}\hat{\mathrm{B}}[T'(t)] \\ \vec{C}_{\vec{u}}\hat{\mathrm{B}}[q'(t)] \\ D_{\vec{u}}\hat{\mathrm{B}}[P'(t)] \end{pmatrix} \tag{5}$$

In the case of a single observation, the matrix $(HMBM^TH^T+R)$ is reduced to a scalar value :

$$HMBM^TH^T + R = \sigma_b^2[\vec{u}'(t+1)] + \sigma_o^2[\vec{u}'(t+1)] \tag{6}$$

On the other hand, if we calculate $HMBM^TH^T$, then we deduce :

$$\sigma_b^2[\vec{u}'(t+1)] = A_{\vec{u}}^2 \cdot \sigma_b^2[\vec{u}'(t)] + \vec{B}_{\vec{u}} \cdot \vec{B}_{\vec{u}} \cdot \sigma_b^2[T'(t)] + \vec{C}_{\vec{u}} \cdot \vec{C}_{\vec{u}} \cdot \sigma_b^2[q'(t)] + \vec{D}_{\vec{u}} \cdot \vec{D}_{\vec{u}} \cdot \sigma_b^2[P'(t)] \tag{7}$$

Thus the operator that transforms the innovation at time $t+1$ to an increment at time t is :

$$\mathrm{B}M^TH^T(HMBM^TH^T + R)^{-1} = \begin{pmatrix} A_{\vec{u}}\hat{\mathrm{B}}[\vec{u}'(t)] \\ \vec{B}_{\vec{u}}\hat{\mathrm{B}}[T'(t)] \\ \vec{C}_{\vec{u}}\hat{\mathrm{B}}[q'(t)] \\ D_{\vec{u}}\hat{\mathrm{B}}[P'(t)] \end{pmatrix} / \left(\sigma_b^2[\vec{u}'(t+1)] + \sigma_o^2[\vec{u}'(t+1)]\right) \tag{8}$$

This equation is equivalent to the following one :

$$\mathrm{B}M^TH^T(HMBM^TH^T + R)^{-1} = \begin{pmatrix} A_{\vec{u}}\hat{\mathrm{B}}[\vec{u}'(t)] / \sigma_b^2[\vec{u}'(t+1)] \\ \vec{B}_{\vec{u}}\hat{\mathrm{B}}[T'(t)] / \sigma_b^2[\vec{u}'(t+1)] \\ \vec{C}_{\vec{u}}\hat{\mathrm{B}}[q'(t)] / \sigma_b^2[\vec{u}'(t+1)] \\ D_{\vec{u}}\hat{\mathrm{B}}[P'(t)] / \sigma_b^2[\vec{u}'(t+1)] \end{pmatrix} \cdot \frac{\sigma_b^2[\vec{u}'(t+1)]}{\left(\sigma_b^2[\vec{u}'(t+1)] + \sigma_o^2[\vec{u}'(t+1)]\right)} \tag{9}$$

The second term in the right-hand-side of (9) corresponds to a stage in the analysis process during which the observed information is filtered; it gives the value of the wind analysis increment $d(u,v)(t+1)$ at the observation point knowing the wind innovation $[y - H(x^b)]_{wind} = \delta(u,v)(t+1)$:

$$d\vec{u}(t+1) = \frac{\sigma_b^2[\vec{u}'(t+1)]}{\left(\sigma_b^2[\vec{u}'(t+1)] + \sigma_o^2[\vec{u}'(t+1)]\right)} \delta\vec{u}(t+1) \tag{10}$$

The first term in the right-hand-side of (9) corresponds to the spatio-temporal multi-multivariate propagation of the filtered information. It indicates how $d(u,v)(t+1)$ is transformed to the analysis increments $dx(t)$ of all state-vector variables (the five variables here) with the adjoint momentum equation.

In 4d-var, unlike 3d-var, there exist an impact (caused by the introduction of the model in the observation operator) of wind observations on the initial conditions for specific humidity, through the adjoint momentum equation. We have :

$$\begin{aligned}
d\vec{u}(t) &= A_{\vec{u}}\hat{\mathrm{B}}\left[\vec{u}'(t)\right] / \sigma_b^2\left[\vec{u}'(t+1)\right] \cdot d\vec{u}(t+1) \\
dT(t) &= \vec{B}_{\vec{u}}\hat{\mathrm{B}}\left[T'(t)\right] / \sigma_b^2\left[\vec{u}'(t+1)\right] \cdot d\vec{u}(t+1) \\
dq(t) &= \vec{C}_{\vec{u}}\hat{\mathrm{B}}\left[q'(t)\right] / \sigma_b^2\left[\vec{u}'(t+1)\right] \cdot d\vec{u}(t+1) \\
dP(t) &= D_{\vec{u}}\hat{\mathrm{B}}\left[P'(t)\right] / \sigma_b^2\left[\vec{u}'(t+1)\right] \cdot d\vec{u}(t+1)
\end{aligned} \tag{11}$$

The complete equation for specific-humidity increments is :

$$dq(t) = \frac{-\hat{\mathrm{B}}[q'(t)]}{\sigma_b^2[\vec{u}'(t+1)]}(R_v - R_d)\left[\int_\eta^1\left(\vec{\nabla}(\ln P) + \frac{\partial \ln P}{\partial \eta}\vec{\nabla}\right)(T\,\bullet)d\eta + T\vec{\nabla}(\ln P)\cdot\bullet\right]\cdot d\vec{u}(t+1) \tag{12}$$

The same approach applied when using a single temperature-observation leads to the following equation :

$$dq(t) = \frac{-\hat{\mathrm{B}}[q'(t)]}{\sigma_b^2[T'(t+1)]}\frac{RT\omega}{PC_p}\left[\frac{R_v - R_d}{R} - \frac{C_{pv} - C_{pd}}{C_p}\right]\cdot dT(t+1) \tag{13}$$

From these equations, we can deduce the following suggestions :

- To reduce the multivariate effects (between specific humidity and other variables), we can try to adjust the background-error standard deviations of specific humidity (decrease them). But in the same time, we must also adjust the corresponding observation-error standard deviations in order to keep the information coming from observations.
- Use more and more observations informing on humidity to avoid a great impact of wind or mass observations on humidity. The anomaly of specific humidity increments shown in my previous papers happened in a region devoid of humidity observations. An experiment consisting in introducing an artificial TEMP observation (created from the guess field) in North-West Spain resolved completely the problem.

Specific humidity increments given by the above equations imply that if 4d-var tries to fit wind observations at time $t+1$ - for example to reduce $d(u,v)(t+1)$ -, it may create a large modification of the initial specific humidity. Thus, the unrealistic increments could appear when, for example, the remaining observations and dynamics (temperature observations and temperature evolution in particular) tend to lead to a modification of initial temperature that does not contribute to a reduction of wind increments (or in contrary tend to amplify them). In that case when adding temperature and pressure observations, specific humidity is excessively amplified.

3. Background specific-humidity error diagnosis (following Rabier et al., 1998)

When studying the background errors at radiance observation points, that appeared to be locally unrealistically large over the West coast of Africa, in an ECMWF 4d-var experiment, Anderson et al. (2000) noticed that this was associated to a maximum of background specific-humidity errors. A simple modification to limit these humidity background errors in very dry areas was developed and tested : arbitrarily limiting the standard deviation of background errors ($\sigma(q)$) to a maximum of 125% of the background field (q), above 800 hPa. In doing so the general features of the humidity background errors were unaltered, but the extremely high values were reduced.

In the ARPEGE/IFS assimilation system, the humidity background errors are not cycled ; the specification of the standard deviations is not derived from the NMC statistics but from statistics of radiosonde observations minus background fields, stratified according to observed temperature and relative humidity. They are modelled as a function of the background temperature T_b and relative humidity Hu_b :

$$\sigma_b(Hu) = -0.002T_b - 0.0033|T_b - 273.| + 0.25Hu_b - 0.35|Hu_b - 0.4| + 0.70,$$
$$\sigma_b(Hu) = \min[0.18, \max(0.06, \sigma_b(Hu))].$$

The standard deviation in terms of relative humidity is then converted to specific humidity, deriving the variations of q from the equation :

$$q = Hu\, e_{sat}(T)/[(R_v/R_d)\cdot P - (R_v - R_d)/R_d \cdot Hu\, e_{sat}(T)],$$

where e_{sat} is the saturation water-vapour pressure, depending on temperature (Tetens' formula) and P is pressure.

Humidity increments are forced to be negligibly small above the tropopause to avoid a systematic drift of stratospheric humidity over extended periods of data assimilation. Humidity in the stratosphere is then mainly driven by the model, and not controlled by observations. This is achieved by setting a very low value (10^{-8}) for $\sigma_b(Hu)$:

- wherever the pressure is lower than 70 hPa,
- at any other point with pressure in the range 70-500 hPa, if the background temperature and pressure fields are such that the square of the buoyancy frequency exceeds $2.10^{-4}\,s^{-2}$ everywhere above that point till 70 hPa.

In addition, any value of $\sigma_b(Hu)$ lower than 10^{-8} is reset to 10^{-8}.

For pressure less than 800 hPa, and over sea, the above model of background errors is modified as :

$$\sigma_{back}(Hu) = \sigma_b[1 - a + a\cdot \exp(-(\Delta P/\beta)^2)], \quad \Delta P = P_b - P_o, \quad a = 0.5(1-LSM),$$

where LSM is the land-sea mask and β=12500 Pa.

Fisher and Courtier (1995) suggested that a randomisation method can be used to diagnose the effective background-error variances and compute matrix B in 3d-var. The method allows the calculation of a low rank estimate of B in terms of model variables in gridpoint space, and is known as randomisation estimate. The method applies to 3d-var, since no account is taken of the evolution of background errors in time. In a 4d-var system, this provides a diagnosis of the effective background errors at the beginning of the assimilation period. This method could be extended to compute an approximation to the background error in terms of observable quantities (Anderson et al., 2000).

This method is applied for the situation of April 24th , 2001, (at 15:00 UTC), in order to diagnose the effective background standard deviations used by 4d-var.

On Fig. 4, one can notice the correspondence between large 4d-var increments and strong STD assigned to both specific and relative humidity (for this situation). This is more visible for low levels (between 500 hPa and the surface).

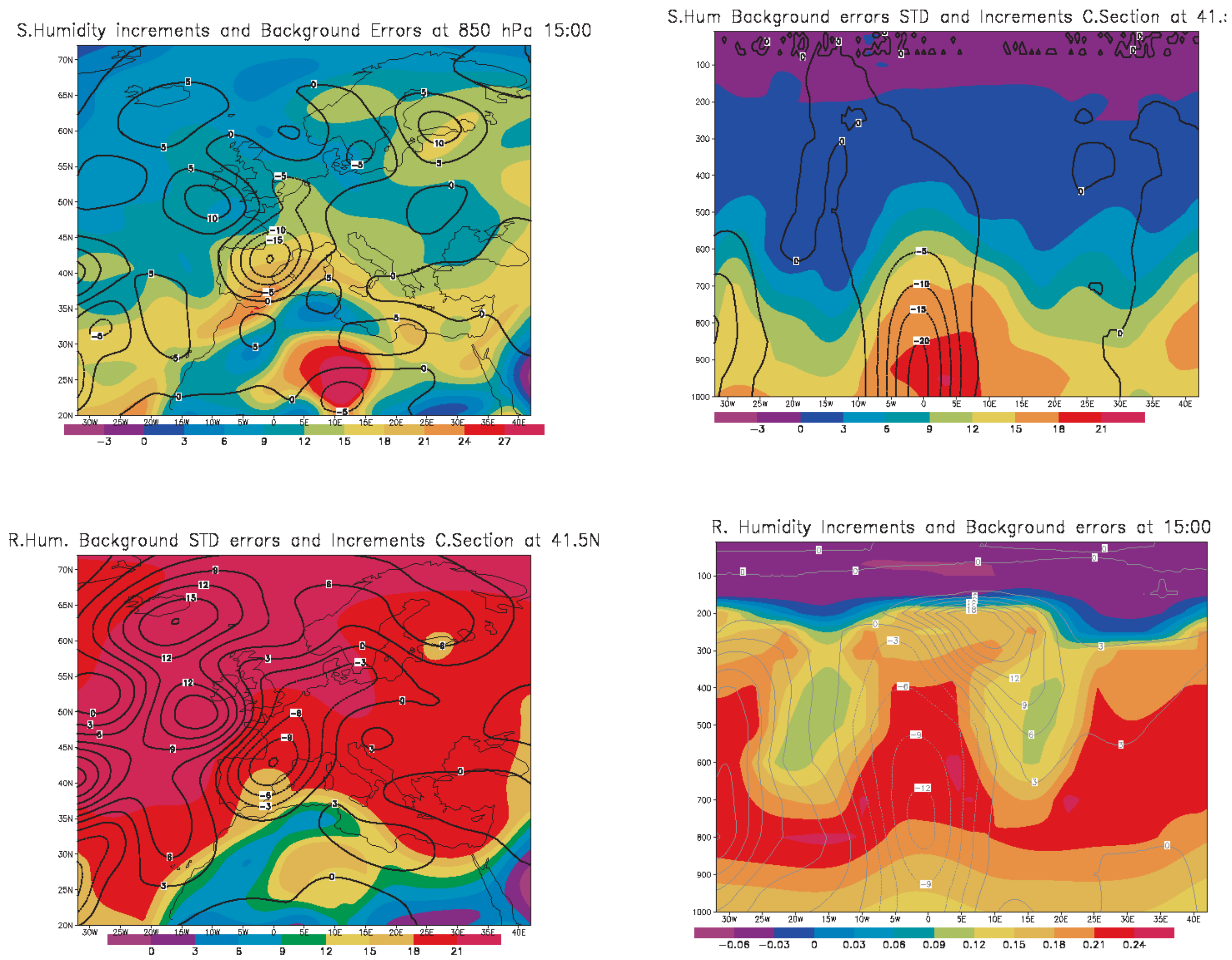

Figure 4: Superimposed standard deviations of background errors (STD, color scale) and 4d-var increments (isolines) at 15:00 UTC for relative humidity (bottom panel) and specific humidity (top panel). The cross-sections on the right are performed at latitude 41.5°N. Specific-humidity values multiplied by 10^4, both for STD and increments. For relative humidity, absolute STD values are mentioned, while increments are in %.

These large background error standard deviations are amplified during the tangent-linear integration along the assimilation window. And this forces 4d-var to remain far from the guess field (as far as specific humidity is concerned) at each time step, because the process of minimization has no other information on humidity except the multivariate information imposed by the remaining analysed fields and their dynamics and observations. In other words, when trying to analyse specific humidity, 4d-var relay on mainly three components :

- humidity observations,
- humidity background,
- multivariate effect.

For the case of April 24th, 2001, the first ingredient does not play any part because over Spain there was no TEMP along the assimilation window. The second ingredient is governed by the magnitude of the background errors assigned to the humidity variable at the beginning of the assimilation window and by the implicit evolution of these quantities during the minimization. The specific atmospheric dynamics (discussed and shown below) is in favour of an amplification of these quantities along the assimilation window. As a consequence, background humidity information is only weakly taken into account. It is then clear that the multivariate effect will predominantly govern alone the behaviour of the analysis of specific humidity.

4. Experimental study of the multivariate terms affecting specific humidity

As shown in a previous paper, the adjoint terms governing the magnitude of the gradient (with respect to specific humidity) are:

$$- \ (R_v - R_d)\left[-\int_{\eta}^{1} \left(\frac{\partial \ln P}{\partial x} + \frac{\partial \ln P}{\partial \eta}\cdot\frac{\partial \bullet}{\partial x}\right)(T\bullet)\,d\eta - T\cdot\frac{\partial \ln P}{\partial x}\bullet \right] Grad(u)$$

$$- \ (R_v - R_d)\left[-\int_{\eta}^{1} \left(\frac{\partial \ln P}{\partial y} + \frac{\partial \ln P}{\partial \eta}\cdot\frac{\partial \bullet}{\partial y}\right)(T\bullet)\,d\eta - T\cdot\frac{\partial \ln P}{\partial y}\bullet \right] Grad(v)$$

$$- \ \frac{RT\omega}{PCp}\left[(R_v - R_d)/R - (Cp_v - Cp_d)/Cp\right] Grad(T)$$

$$- \ \left[\dot{\eta}\frac{\partial \bullet}{\partial n} + u\frac{\partial \bullet}{\partial x} + v\frac{\partial \bullet}{\partial y}\right] Grad(q)$$

The two first terms corresponds to the wind information that will act on humidity. For instance, *Grad(u)*, which contains mainly the contribution of wind observations, will affect humidity in a proportion depending on the tendency and magnitude of the term between brackets. If 4d-var tends to decrease wind gradient (wind increments) to fit wind observations, whereas the dynamics (of mainly temperature and pressure) does not allow that (i.e. terms between brackets remain large at each time step), then 4d-var has only one choice : to act on humidity.

When studying the above first three terms, it appears that their magnitude is governed by the following quantities :

$(R_v - R_d)\, T/P\, \partial_x P$, $(R_v - R_d)\, T/P\, \partial_y P$, and $RT/Cp\ \omega/P[(R_v - R_d)/R - (Cp_v - Cp_d)/Cp] \approx 2/49 R_v/R_d\, T\omega/P$

The common term contributing the most in these three expressions is T/P. This leads us to expect large magnitudes in regions characterized by :

- high temperatures (Sahara, continental regions during summer),
- low pressures (e.g. Saharan low pressures : "dépressions sahariennes"),
- high horizontal pressure gradients (mountainous areas),
- high vertical velocities (mountainous areas).

The term T/P is proportional to $1/\rho$ (ρ being the air density). That means that we could expect bad specific humidity analysis in regions devoid of humidity observations and characterized by small air density. A first try to solve the problem is to decrease specific humidity increments in areas with small ρ.

The following figures give the magnitude of some relevant above-mentioned terms.

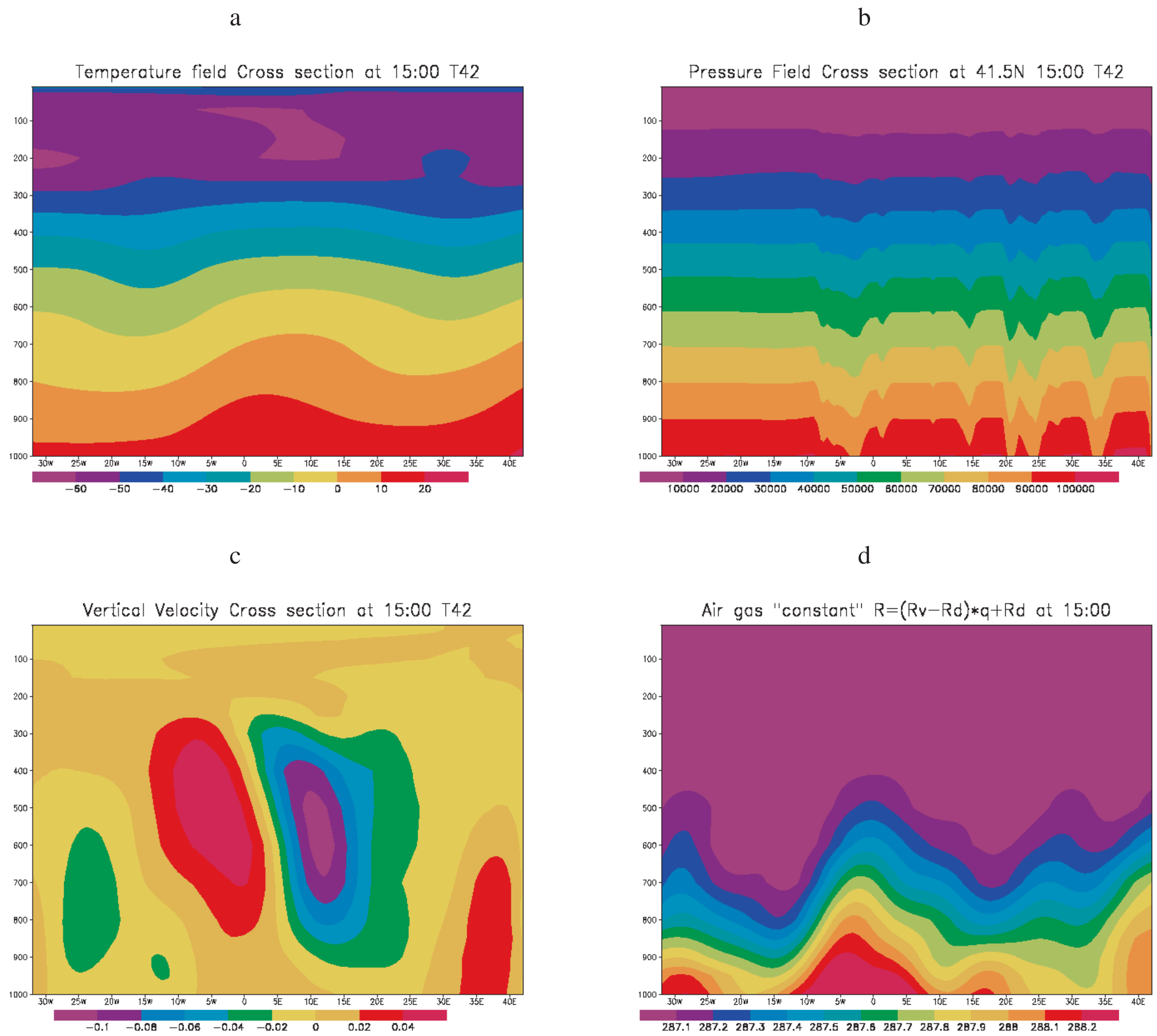

Figure 5: Vertical cross-sections at latitude 41.5°N for : a) temperature, b) pressure, c) vertical velocity, d) air gas constant. One can notice high temperatures, low pressures, high vertical velocities and high *R* values between longitudes -5° and +5°E.

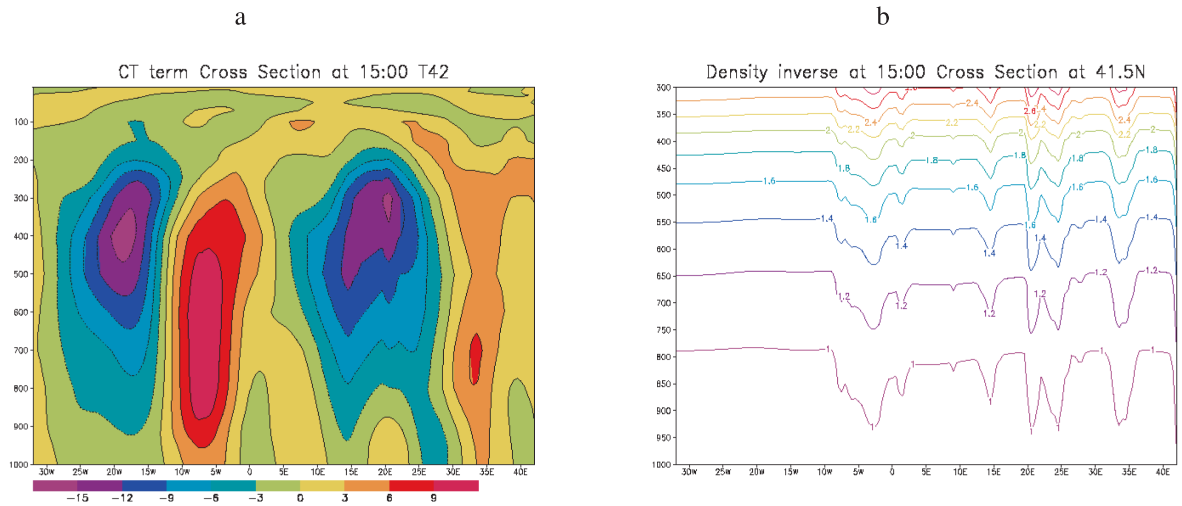

Figure 6 : *CT* term on (a) is the dynamics term coupling temperature observations and specific humidity increments (cf. 4.). This term presents a maximum on a vertical column between 900 hPa and 500 hPa slightly at the west of our area of interest. This corresponds on (b) to relatively high values of density inverse (the corresponding cross section is truncated at 300 hPa).

Figure7 hereafter, by comparison with Fig.5, informs on dynamics, showing the time-evolution of some characteristic fields between 15:00 and 18:00 UTC.

a

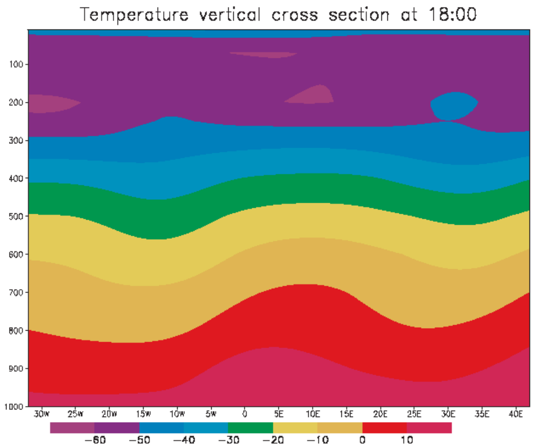

b

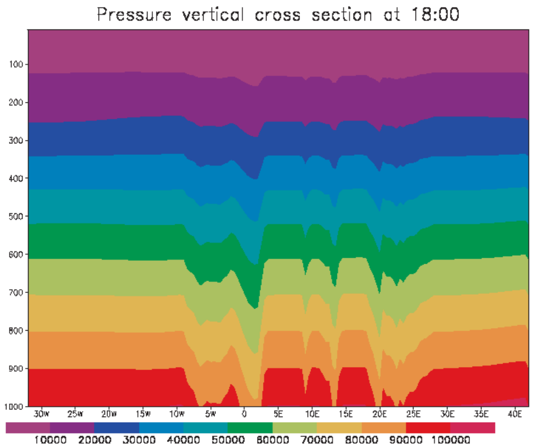

c

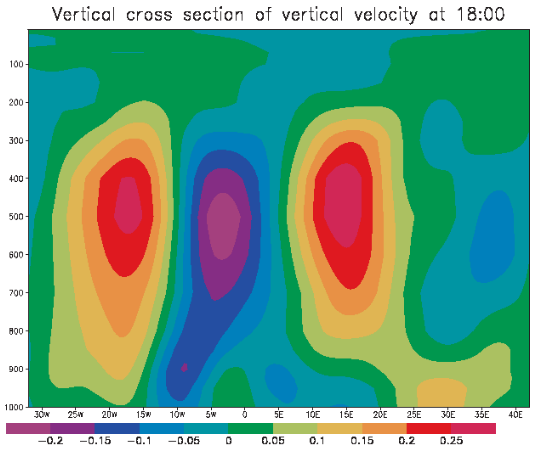

d

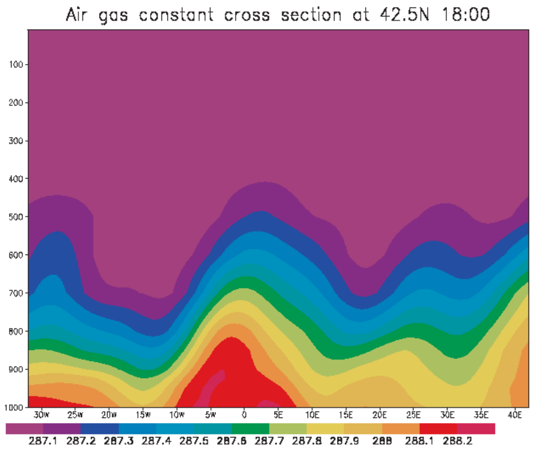

Figure 7: Same as figure 5 at 18:00 UTC.

5. References

Anderson, E., and M. Fisher, 1999 : Background errors for observed quantities and their propagation in time. pp. 81-90 in *Proceedings of the ECMWF workshop on diagnosis of data assimilation systems*, Reading, UK, 1-4 November 1998.

Anderson, E., M. Fisher, R. Munro and A. McNally, 2000 : Diagnosis of background errors for radiances and other observable quantities in a variational data assimilation scheme, and the explanation of a case of poor convergence. *Q. J. R. Meteorol., Soc.*, **126**, pp. 1455-14

Buizza, R., 1994: Sensitivity of optimal unstable structures. *Q. J. R. Meteorol. Soc.*, **120**, 429-451

Daley, R., 1991 : Atmospheric Data Analysis. Cambridge Atmospheric and Space Science Series, Cambridge University Press. ISBN 0-521-38215-7, 457 pages.

Fisher, M., and P. Courtier, 1995 : Estimating the covariance matrices of analysis and forecast error in variational data assimilation. *ECMWF Tech. Memo. 220*. Available from ECMWF, Reading, UK.

Janiskova, M., J.-N. Thépaut and J.-F. Geleyn, 1999 : Simplified and regular physical parameterisations for incremental four-dimensional variational assimilation. *Mon. Wea. Rev.*, **127**, 26-45.

Jazwinski, A.H., 1970 : Stochastic processes and filtering theory. Academic Press.

Lorenc, A., 1986 : Analysis methods for numerical weather prediction. *Quart. J. Roy. Meteor. Soc.*, **112**, 1177-1194.

Mahfouf, J.-F., R. Buizza and R.M. Errico, 1997 : Strategy for including physical processes in the ECMWF data assimilation system. In *Proceedings of the ECMWF Workshop on non-linear aspects of data assimilation*, Shinfield Park, Reading, RG2 9AX, 9-11 September 1996.

Rabier, F., A. McNally, E. Anderson, P. Courtier, P. Unden, J. Eyre, A. Hollingsworth and F. Bouttier, 1998a. The ECMWF implementation of three-dimensional variational assimilation (3D-Var). II: Structure functions. *Q.J.R.Meteorol. Soc.*, **124**, 1809-1829.

Thépaut, J-N., P. Courtier, G. Belaud and G. Lemaître, 1996 : Dynamical structure functions in a four-dimensional variational data assimilation: A case-study. *Q.J.R.Meteorol. Soc.*, **122**, 535-561.

7. Appendix : background standard deviations obtained by randomization vectors technique for surface pressure, temperature, specific humidity on low atmospheric model levels

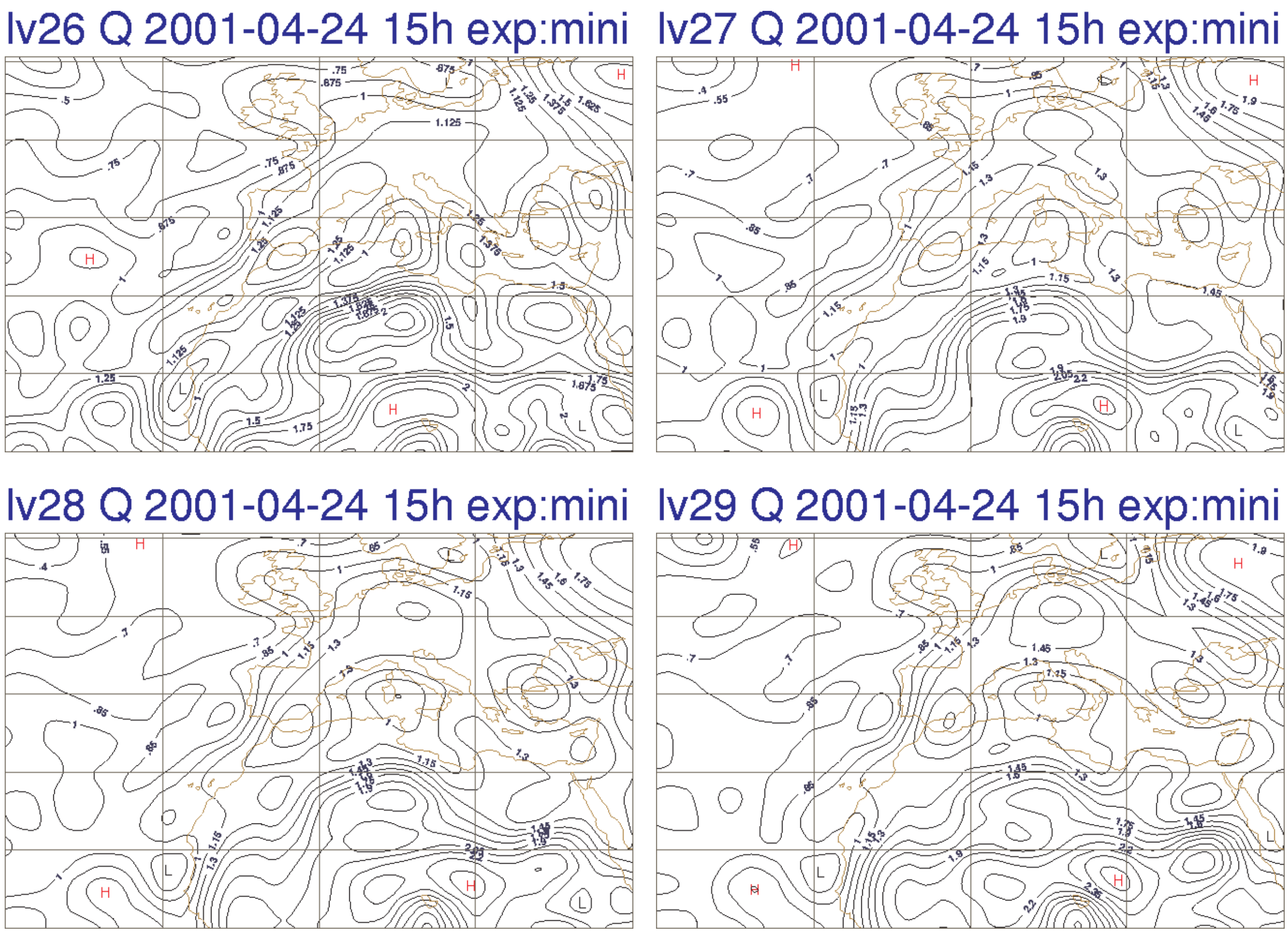

lv30 Q 2001-04-24 15h exp:mini

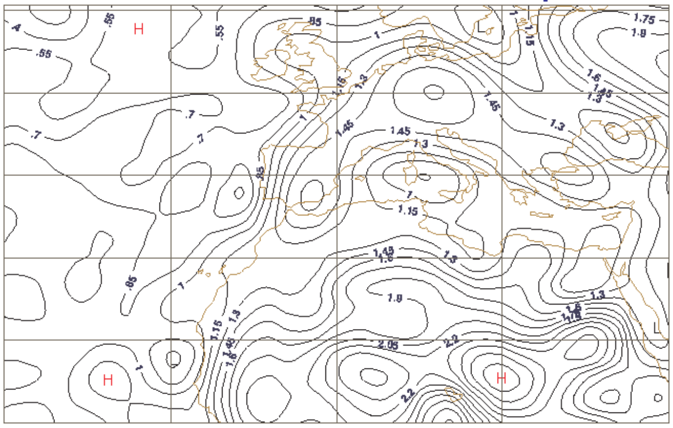

lv31 Q 2001-04-24 15h exp:mini

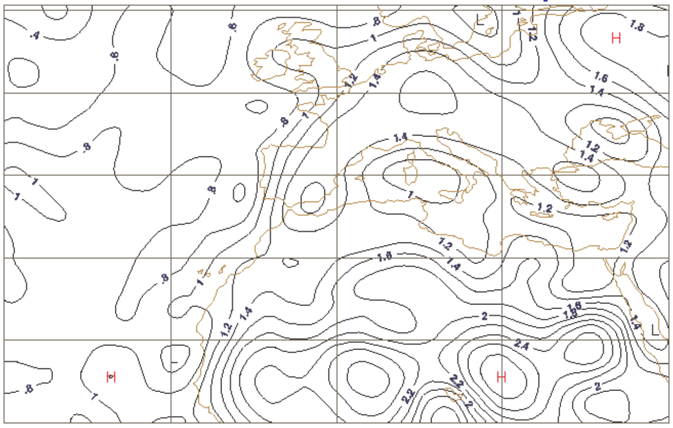

lv25 T 2001-04-24 15h exp:mini

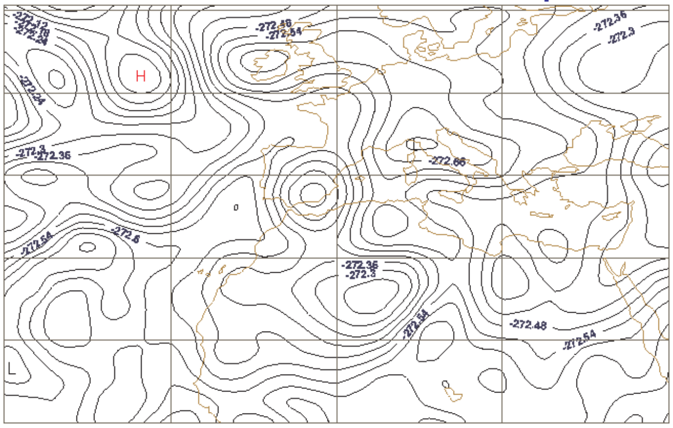

lv27 T 2001-04-24 15h exp:mini

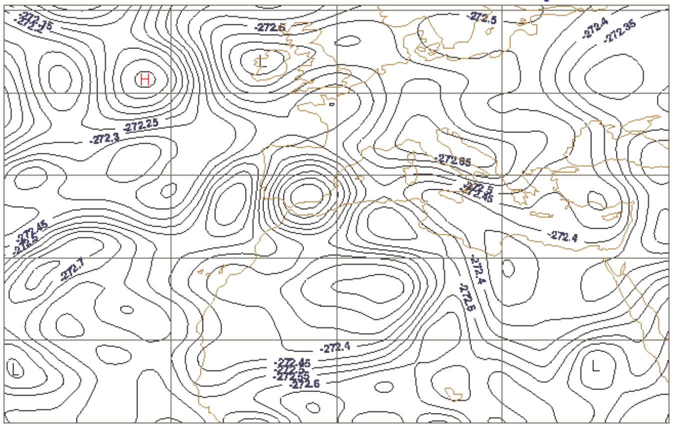

lv28 T 2001-04-24 15h exp:mini

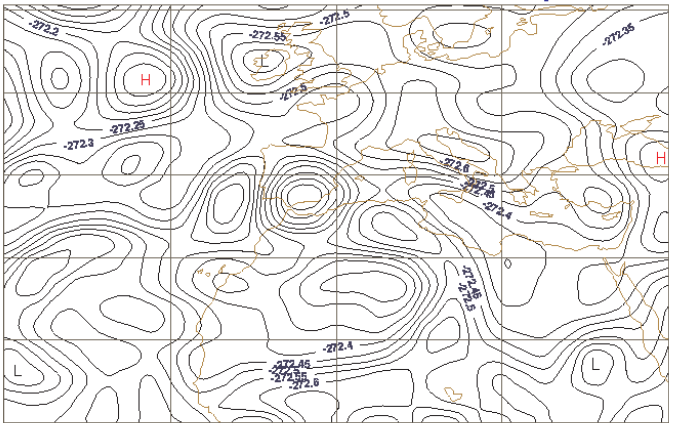

lv1 LNSP 2001-04-24 15h exp:mini